Mater. Res. Soc. Symp. Proc. Vol. 918 © 2006 Materials Research Society 0918-H04-03

Phase Change Materials - From Structures to Kinetics

Matthias Wuttig, Wojciech Welnic, Ralf Detemple, Henning Dieker, Johannes Kalb, Daniel Wamwangi, and Christoph Steimer
I. Physikalisches Institut IA, Aachen, D52056, Germany

ABSTRACT

Phase change materials possess a unique combination of properties which include a pronounced property contrast between the amorphous and crystalline state, i.e. a high electrical and optical contrast. In particular the latter observation is indicative for a considerable structural difference between the amorphous and crystalline state. At the same time the crystallization of the amorphous state proceeds on a fast time scale. This raises the question how structure, properties and kinetics are related in phase change alloys. It will be demonstrated that only a small group of covalent semiconductors with octahedral-like coordination has the required property combination. This is related to their thermodynamic properties which govern the kinetics of crystallization.

INTRODUCTION

Phase change materials are very promising materials for information technology. They are already employed in rewriteable optical data storage, where the pronounced difference of optical properties between the amorphous and crystalline state is used for data storage. This unconventional class of materials is also the basis of storage concepts to replace flash memory [1-3, 4, 5]

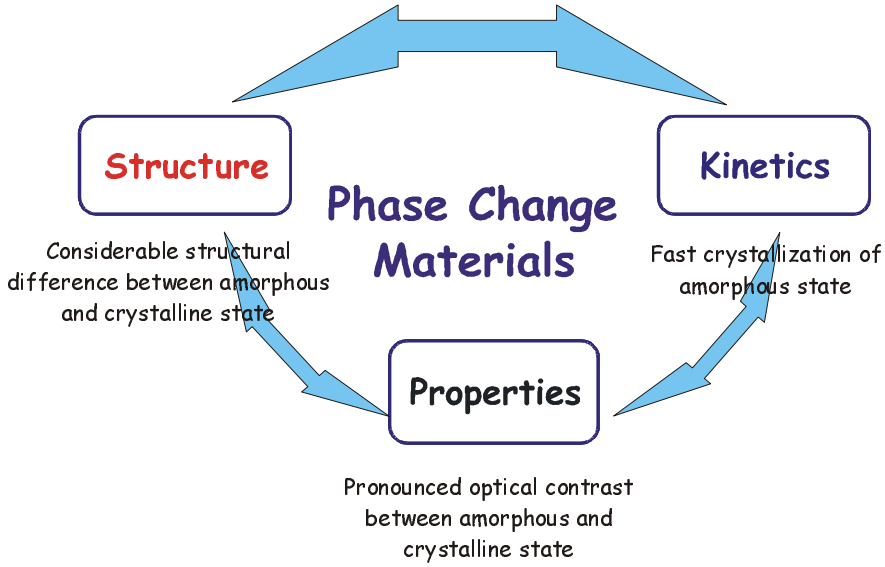

Figure 1. Phase change materials show a unique combination of properties. On the one hand side they display a pronounced contrast of optical and electrical properties between the amorphous and crystalline state as well as threshold switching. The former observation is indicative for a pronounced structural difference between the amorphous and crystalline state. At the same time the crystallization of the amorphous state proceeds on a very short time scale. To exploit the full potential of phase change materials it is important to unravel the origin of this unique property combination and to identify the materials which possess these properties.

This raises the question which material properties are crucial for these storage applications, and which compounds posses the required properties. Successful phase change alloys are characterized by a unique property combination which is depicted in fig. 1. On the one hand side they possess a pronounced contrast of optical properties (reflectivity, transmission) between the amorphous and crystalline state. The corresponding dielectric functions, i.e. ε_1 and ε_2 are displayed in fig. 2 for $Ge_2Sb_2Te_5$, a prototype phase change alloy. The pronounced optical contrast displayed is a unique and rather rare property. Conventional semiconductors such as GaAs or Si are characterized by a much smaller difference in optical properties. Hence we need to understand what causes the property contrast in phase change alloys. The only plausible explanation is a considerable structural difference between the amorphous and crystalline state. Such a different atomic arrangement could lead to different electronic states which should give raise to different optical properties.

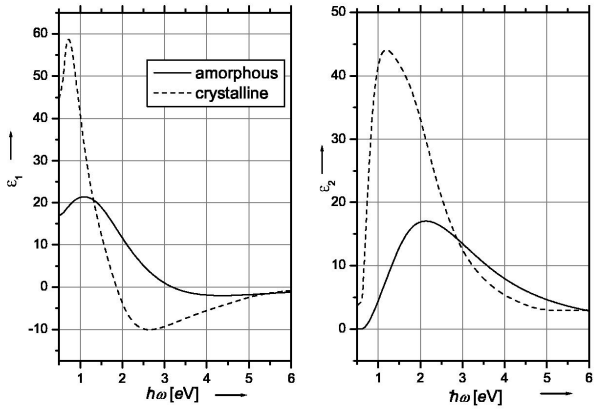

Figure 2. Real and imaginary part of the dielectric constants ε_1 and ε_2 for $Ge_2Sb_2Te_5$, a prototype phase change material, in the amorphous and crystalline state. Note the pronounced difference in amplitudes in ε_1 and ε_2 and the larger bandgap in the amorphous state which is visible in ε_2.

STRUCTURE AND PROPERTIES

In the following we will hence investigate the structural properties of phase change alloys. However, optical contrast alone is not sufficient. In data storage speed, i.e. fast structural rearrangements, are also a must. In phase change recording, crystallization times of a few ns have indeed been observed. While fast crystallization alone is not uncommon and certain materials are known for their fast crystallization processes, it is more difficult to understand how crystallization can be fast in materials where the atomic arrangement in the amorphous and crystalline state is very different. In the following we will therefore start by discussing the structural properties of typical phase change alloys.

Figure 3 displays selected area diffraction patterns for a crystalline bit in an amorphous matrix. The patterns demonstrate that the amorphous surrounding of the crystalline bits does not possess long range order, while the crystalline bit shows long range order characteristic for a rocksalt-like structure. This observation alone however can not explain the pronounced optical contrast since qualitatively similar patterns could also be recorded if e.g. Si or SiO_2 would be locally crystallized. Hence the investigation of the short range order of both phases is mandatory as well. Recently Kolobov et al. have provided interesting EXAFS data for $Ge_2Sb_2Te_5$ which reveal an amazing structural difference between the amorphous and crystalline state [8]. The most noteworthy structural change is a rearrangement of the Ge atom from an octahedral site in the crystalline state to a tetrahedral site in the amorphous state.

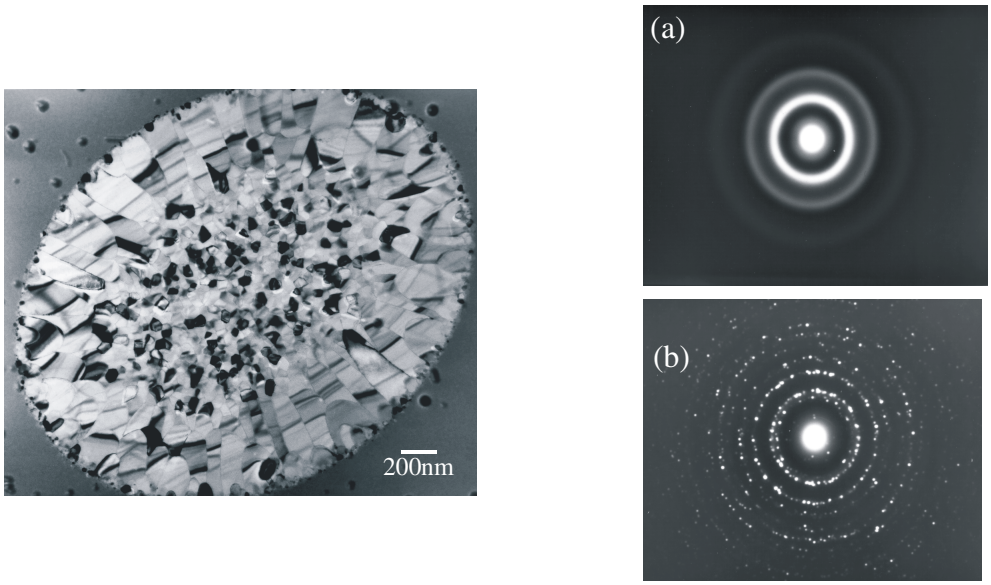

Figure 3. TEM image of a laser-crystallized spot in an uniform grey background [6]. The corresponding Selected Area Diffraction Patterns of the amorphous a) and crystalline region b) clearly indicate the absence and presence of long range order as evidenced by the broad rings and sharp spots, respectively.

We have therefore employed density functional theory to determine the relationship between structure and energy for a typical phase change alloy [7]. For these calculations we have used $Ge_1Sb_2Te_4$. Such as material shares many properties that are characteristic for phase change alloys with the prototype material $Ge_2Sb_2Te_5$. At the same time this alloy is much better suited for density functional theory calculations since it can be described with a much smaller unit cell. To determine the atomic arrangement in $Ge_1Sb_2Te_4$ a number of different atomic arrangement has been considered. They include the chalcopyrite structure where every atom is tetrahedrally coordinated, the rocksalt phase and the spinel structure where Ge has four nearest neighbours and Sb and Te are octahedrally coordinated. The resulting energy as a function of lattice size is displayed in fig. 4. It can be seen that the chalcopyrite structure has both a much larger lattice constant and a higher energy than the structures with the lowest energy. Hence this phase will not be adopted in phase change alloys. The lowest energy is found for a distorted rocksalt structure where shorter and longer Ge-Te as well as Sb-Te bonds are formed. Such a distortion pattern is characteristic for a Peierls-like distortion. The second best atomic arrangement is found for the spinel structure, where Ge atoms have a tetrahedral coordination. This is in line with the EXAFS analysis by Kolobov et. al. [8], who observed a tetrahedral arrangement of Ge atoms in the amorphous state. The density of this phase is lower, as can be seen from figure 4. The quantitative difference between these two phases is around 30 meV, in good agreement with the observed heat of crystallization [9].

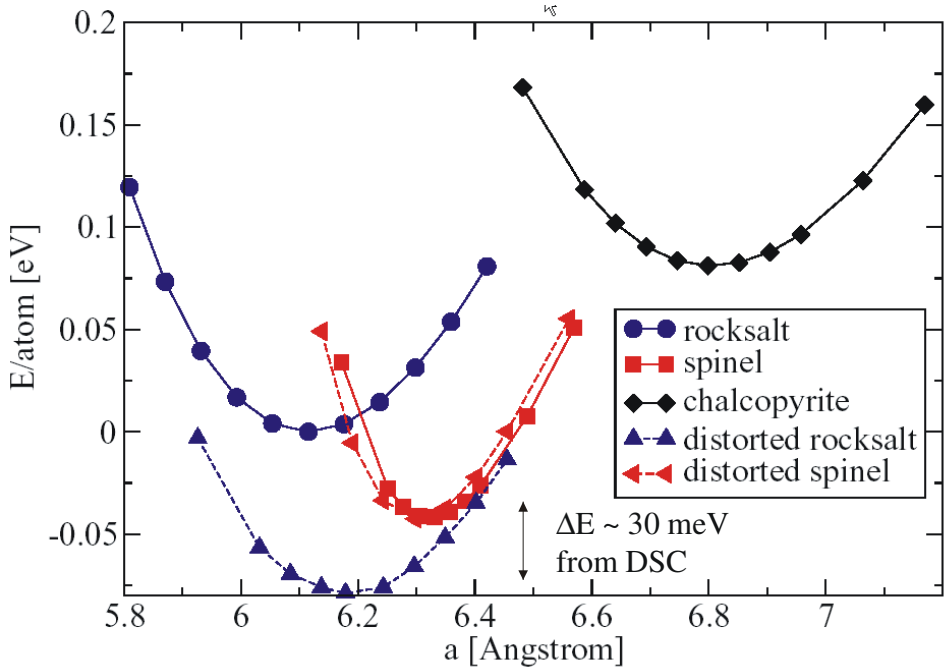

Figure 4. Ground-state energy vs. lattice constant for the ideal and relaxed rock salt -, spinel - and chalcopyrite structure. Due to its negligible energetic and structural relaxation the ideal chalcopyrite values are shown only. The energy difference and lattice expansion between the lowest energy (distorted rocksalt) and the second best structure, the spinel phase are in good agreement with experimental values for the difference between the crystalline and amorphous phase [9].

Note that the spinel structure we use to model the amorphous state in the DFT calculations still possesses long range order, since our unit cell only contains 56 atoms. Yet the pronounced optical contrast that is characteristic for phase change alloys must be related to differences in the short range order between the amorphous and crystalline state. Such differences can be reasonably well described employing medium size unit cells. Hence the most pronounced difference between the two phase, i.e. the distorted rocksalt structure describing the metastable crystalline state and the spinel structure describing the atomic arrangement in the amorphous structure is the arrangement of the Ge atom. This raises questions regarding the range of stoichiometries which show the characteristic properties of phase change alloys.

Before this issue is addressed, figure 5 displays the difference in the density of states between the rocksalt and the spinel structure. This difference is e.g. responsible for the optical contrast between both states. It is noteworthy that a significant change of states is observed close to the Fermi energy. This change is mainly caused by differences in the p-states of Te, even though Ge atoms are shifted the most if we compare the arrangement in the rocksalt and spinel structure. The Ge atoms switch from an octahedral – like arrangement in the rocksalt structure to a tetrahedral arrangement in the spinel phase. This implies that phase change alloys are characterized by a structural instability, where both atomic arrangements have similar energies. Therefore the question needs to be settled which alloys show such a structural instability. In figure 6 the ground state energy a number of Te alloys is displayed [10].

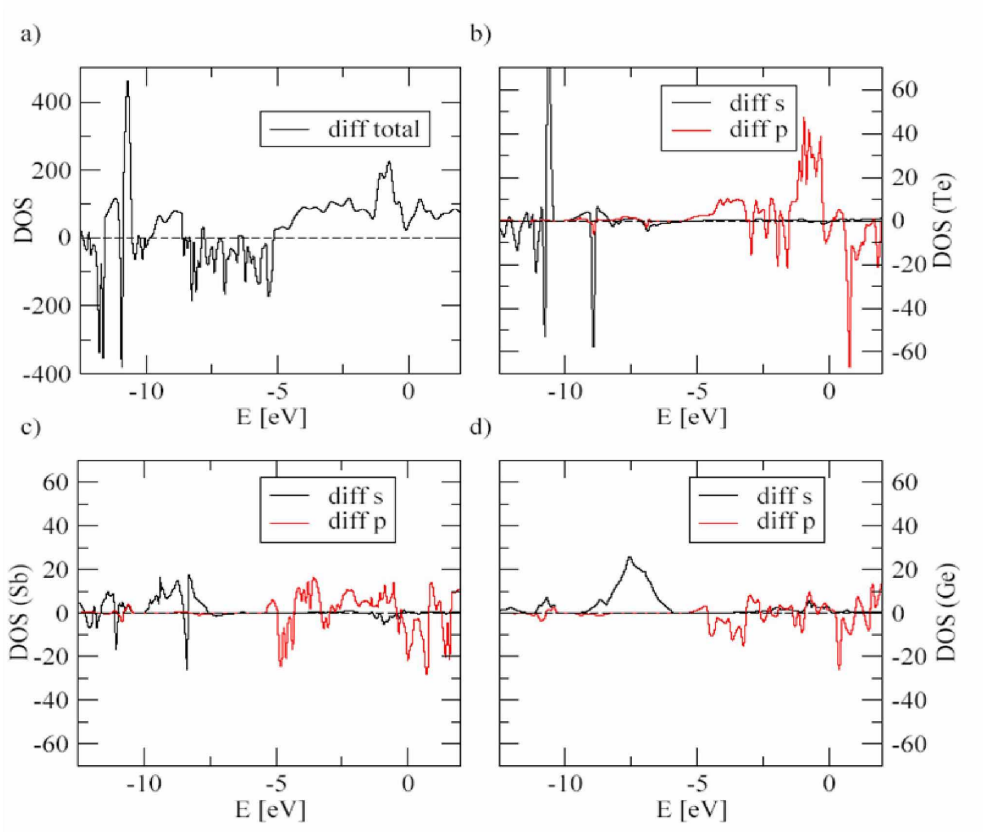

Figure 5. Difference of the density of states between the relaxed rock salt -and spinel structures for all atoms and for the s-and p-bands for each element. The difference of the overall density of states shows an increase just below the Fermi-level (0 down to −5 eV), which should be responsible for the optical contrast in the visible range observed on crystallisation. The difference in the density of states can be attributed mostly to the p-orbitals of Te, as Ge shows a broad change in the s-band well below the energies relevant for the optical properties only, but small differences in the p-band. The changes in the Sb s-and p-band are in between the extremes Ge and Te.

Once the alloy has more than four valence electrons the ground state is octahedral. Only for Te alloys with an average number of four valence electrons a tetrahedral atomic arrangement, i.e. a chalcopyrite structure is predicted for the crystalline state. This is presumably related to the ideal filling of the bonding state of the chalcopyrite structure if an average number of 4 valence electrons is available. Once more than 4 valence electrons have to be distributed, the antibonding states of the chalcopyrite lattice start to the occupied, which destabilizes the structure. Hence for more than 4 valence electrons the rocksalt like crystalline structure becomes favourable. For these materials the characteristic features of phase change alloys are found. This implies that only a subset of Te alloys, i.e. those with an octahedral-like arrangement in the crystalline state show the desired property combination of phase change alloys.

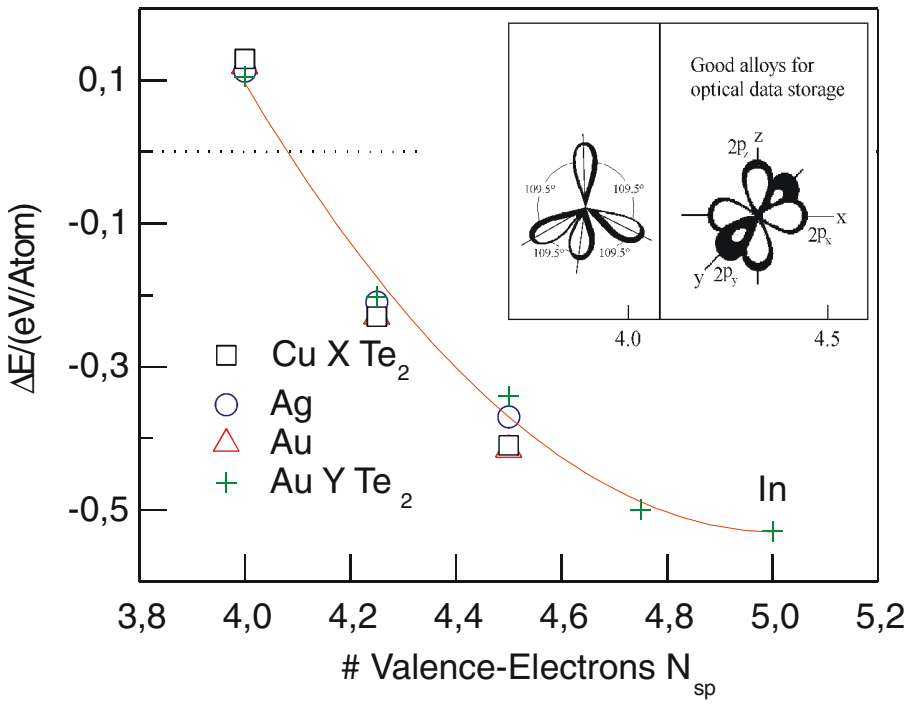

Figure 6. Energy difference between rocksalt -and chalcopyrite structure, calculated by DFT for different model-alloys with varying number of valence electrons but constant ratio of constituents. X = Cd, In, Sn, Sb; Y = Ga, Ge, As, Sb; see [10] for details.

KINETICS

As discussed in the opening section, phase change alloys are characterized by a unique property combination which includes rapid crystallization processes. In typical phase change alloys crystallization or better re-crystallization as sketched below, proceeds on a nanosecond time scale. Hence it is important to understand, why and for which materials such fast crystallization phenomena are to be expected. Crystallization is a well understood process that is controlled by the competition of nucleation, i.e. the formation of crystalline grains in an amorphous matrix and subsequent growth. The easiest way to visualize the efficiency of crystallization as a function of temperature is in Time-Temperature-Transformation diagrams such as figure 7.

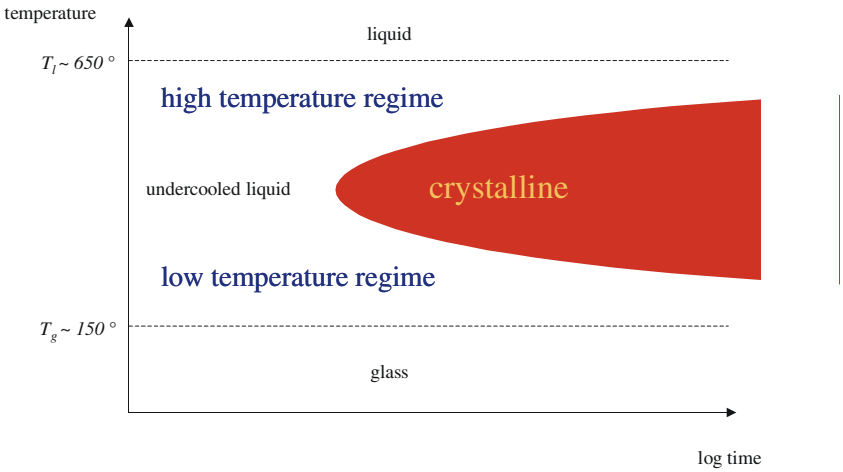

Figure 7. Time Temperature Transformation (TTT) diagram for crystallization.

Typically crystallization is slow just below the melting temperature where the driving force for nucleation is small, but atomic mobilities are large. On the other hand, crystallization is also slow for low temperatures close to T_g, where the driving force for crystallization is high

but atomic mobilities are low. Hence the fastest crystallization processes are observed at intermediate temperature (nose of the TTT-diagram), where both the driving force and the atomic mobility are moderately high. While this behaviour is conceptionally well understood, it is very challenging to determine the required experimental parameters that describe crystallization for a wide temperature range. One reason is related to the speed of crystallization. In a typical phase change alloy crystallization proceeds on a nanometer length and nanosecond time scale. This makes precise measurements at well known temperatures almost impossible. Hence the extrapolation of properties becomes a necessity. Frequently measurements close to T_g are performed and used to predict the behaviour at higher temperatures.

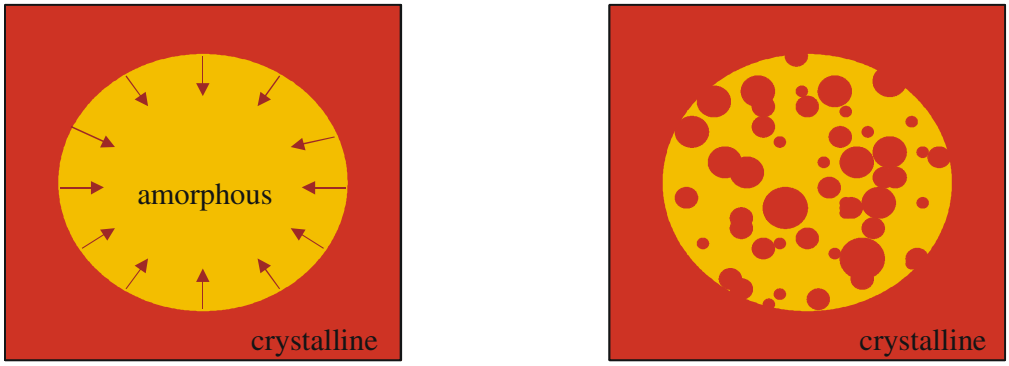

Figure 8. Growth dominated re-crystallization as observed for AgIn-doped Sb_2Te and $Ge_{12}Sb_{88}$ (left) compared to nucleation-dominated re-crystallization for $Ge_4Sb_1Te_5$ and $Ge_2Sb_2Te_5$ (right).

Depending on whether crystallisation is dominated by the rapid formation of a comparatively large number of crystalline nuclei that grow to smaller crystals or the fast growth of a smaller number of crystals to larger crystals the material is referred to as a nucleation - or growth-dominated material. Figure 8 sketches the re-crystallization of an amorphous bit in a crystalline matrix and illustrates both crystallization mechanisms. In the case of a growth dominated material, the amorphous spot is re-crystallized from the crystalline rim before crystalline nuclei are formed. For the nucleation dominated material the formation of crystalline nuclei is faster than the growth of the crystalline matrix resulting in more but smaller crystals [11-14].

Phase change materials showing these different recrystallization mechanisms have been observed experimentally by Atomic Force Microscopy (AFM). Thin films of phase change materials on a substrate were annealed in an oil-bath at temperatures around T_g, i.e. on the low temperature side of the crystallization nose of the TTT-diagram (figure 7). Crystallization is then stopped by removing the samples from the oil and transferring them to an AFM. Crystallization and the densification involved show up as a height contrast in the AFM. Thus the number of crystals and their size can be tracked as a function of annealing temperature and by putting the samples back and forth to the oil-bath also as a function of annealing time. Comparing the size of the crystals in subsequent pictures taken at the same temperature, the growth velocity can be determined. If the experiment is repeated at different temperatures, the activation energy for crystal growth can be determined from an Arrhenius-plot as given on the left half of figure 9 [15]. Apparently for the temperature range studied the growth velocity of the three different alloys shows similar activation energies. The number of crystals observed

as a function of annealing temperatures is shown in the right half of figure 9. While the density of crystals increases for the GeSbTe-based materials, it remains constant for AgIn-doped Sb_2Te.

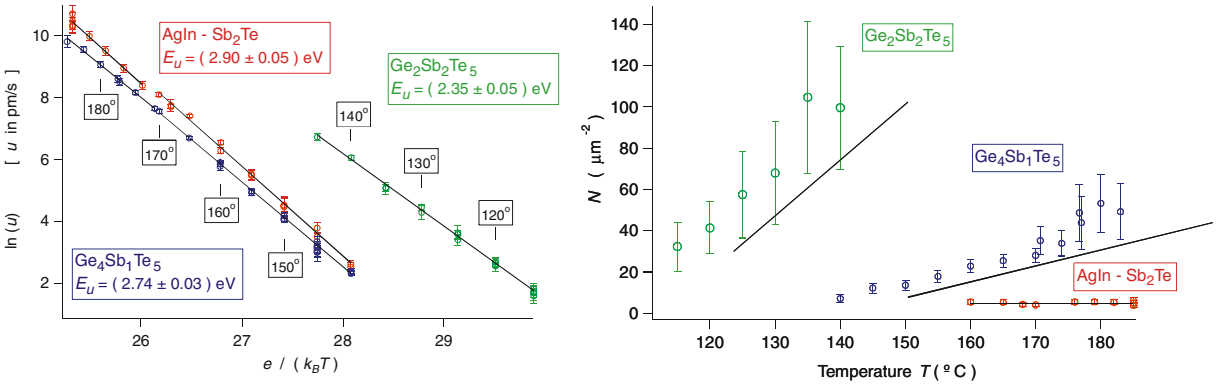

Figure 9. Growth-velocity (left) and density of crystals from AFM-measurements for nucleation - and growth-dominated materials. While the activation energy for growth in the Arrhenius-plot on the left is similar, the crystal density shows a completely different behaviour.

Thus the AFM-pictures allow a direct distinction between nucleation - and growth dominated materials i.e. GeSbTe alloys and AgIn-doped Sb_2Te. The similar activation energies in the left hand side in combination with the constant number of nuclei for AgIn-doped Sb_2Te in the right hand side of figure 9 show, that it is a reduced nucleation rate rather than an increased growth speed that distinguishes both re-crystallization mechanisms. Yet, this study does not provide the insight which microscopic parameter is responsible for the different behaviour. Nucleation involves the build-up of an interface between the crystalline nucleus and the surrounding matrix. With the dependence of the nucleation rate on the ratio of the glass and liquidus temperature, viscosity and melting entropy known [16], this surface energy is the last crucial parameter to be determined. Hence we have performed undercooling experiments on phase change alloys, approaching crystallization from the high temperature regime of figure 7 [16]. With the other parameters known, a minimum value for the interfacial energy between the crystalline nucleus and the liquid matrix can be determined from the maximum undercooling observed in a calorimeter. To prevent crystallization from the solid walls of a crucible, the samples were surrounded by a B_2O_3-flux that does not show any phase transitions in the temperature range from 440 to 720 °C used in our Differential Scanning Calorimetry experiments (DSC) and provides a liquid sample container. Additionally B_2O_3 serves as a solvent for possible impurities as the samples were fluxed beyond their melting point for purification before the actual undercooling experiments. Undercooling was determined from the inset of the exothermic heat of crystallization.

Table 1. Lower limit for the combined interfacial energy and entropy of fusion $\alpha^3\,\beta$. Materials with higher values of that combined energy are slow in nucleation because of the large energy costs of the interface between crystal and liquid.

	$\alpha^3 \cdot \beta$
$Ge_{12}Sb_{88}$	0.024
AgIn-Sb_2Te	0.017
$Ge_4Sb_1Te_5$	0.016
$Ge_2Sb_2Te_5$	0.008

Table 1 gives the results obtained from these undercooling experiments (see [16] for details). The key parameter for the nucleation rate is the product $\alpha^3 \beta$ with α the interfacial energy in units of the enthalpy of fusion and β is the entropy of fusion (all energies per atom). As the nucleation rate depends on the third power of the interfacial energy nucleation is mostly governed by α. Although the values for AgIn doped Sb_2Te and $Ge_4Sb_1Te_5$ are to close to be distinguished without doubt, there is a clear trend towards reduced values of $\alpha^3 \beta$ for nucleation dominated materials as $Ge_2Sb_2Te_5$ as compared to growth dominated alloys as $Ge_{12}Sb_{88}$.

Therefore the values of $\alpha^3 \beta$ in table 1 explain the different nucleation behaviour of GeSbTe-based and AgIn-doped Sb_2Te on an atomistic base. While these values mostly describe the interfacial energy between the undercooled liquid and the stable (hexagonal) phase it is still reasonable to assume, that both phases are fairly comparable to the amorphous and the rocksalt-phase, respectively. Hence these values also provide valuable insight into the reason for the different behaviour encountered upon crystallization of phase change films.

ACKNOWLEDGEMENTS

Financial support by the 6th Framework Program of the European Commission within the CAMELS-Project (contract number IST-3-017406) is gratefully acknowledged.

REFERENCES

1. S. Ovshinsky: *Phys. Rev. Lett.* **21**, 1453 (1968).
2. G.-F. Zhou, *Mat. Sci. and Eng*. **A 304-306**, 73-80 (2001).
3. M. Wuttig, *Nature Materials* **4**, 265 (2005).
4. N. Yamada, *MRS Bulletin* **21**, 48-50 (1996).
5. M. Lankhorst and B. Ketelaars and R. Wolters, *Nature Materials* **4**, 347 (2005).
6. I. Friedrich and V. Weidenhof and S. Lenk and M. Wuttig, *Thin Solid Films* **38**, 389 (2001).
7. W. Welnic, A. Pamungkas, R. Detemple, C. Steimer, S. Blügel and M. Wuttig, *Nature Materials* **5**, 56 (2006).
8. A. Kolobov, P. Fons, A. Frenkel, A. Ankudinov, J. Tominaga and Tomoya Uruga, *Nature Materials* **3**, 703 (2004).
9. M. Klein, *Diploma Thesis RWTH Aachen* (2006) and to be published.
10. M. Luo and M. Wuttig, *Advanced Materials* **16**, 439 (2004).
11. J. Coombs, A. Jongenelis, W. van Es-Spiekman and B. Jacobs, *J. Appl. Phys.* **78**, 4918 (1995).
12. H. Borg, M. van Schijndel, J. Rijpers, M. Lankhorst, G. Zhou, M. Dekker, I. Ubbens and M. Kuijper, *Jpn. J. Appl. Phys*. H. J. Borg et al., *Jpn. J. Appl. Phys*. **40**, 1592 (2001).
13. V. Weidenhof, I. Friedrich, S. Ziegler and M. Wuttig, *J. Appl. Phys*. **89**, 3168 (2001).
14. L. van Pieterson, M. van Schijndel, J. Rijpers and M. Kaiser, *Appl. Phys. Lett.* **83**, 1373 (2003).
15. J. Kalb, F. Spaepen and M. Wuttig, *Appl. Phys. Lett*. **84**, 5240 (2004).
16. J. Kalb, C. Wen, F. Spaepen. H. Dieker and M. Wuttig, *J. Appl. Phys.* **98**, 54910 (2005).